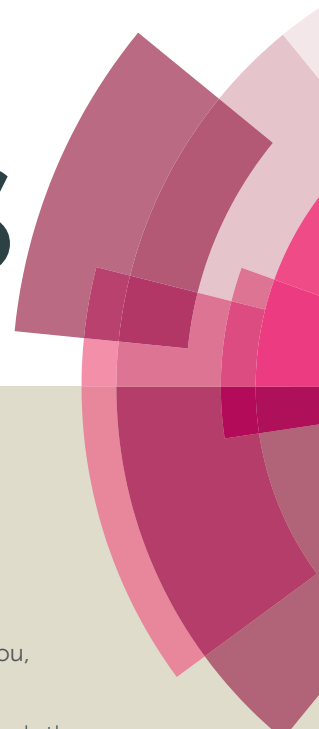


RSC Advances



This article can be cited before page numbers have been issued, to do this please use: L. Zhang, X. Zhou, H. Huo, W. Li, F. Li and R. Li, *RSC Adv.*, 2015, DOI: 10.1039/C5RA07765F.



This is an *Accepted Manuscript*, which has been through the Royal Society of Chemistry peer review process and has been accepted for publication.

Accepted Manuscripts are published online shortly after acceptance, before technical editing, formatting and proof reading. Using this free service, authors can make their results available to the community, in citable form, before we publish the edited article. This *Accepted Manuscript* will be replaced by the edited, formatted and paginated article as soon as this is available.

You can find more information about *Accepted Manuscripts* in the [Information for Authors](#).

Please note that technical editing may introduce minor changes to the text and/or graphics, which may alter content. The journal's standard [Terms & Conditions](#) and the [Ethical guidelines](#) still apply. In no event shall the Royal Society of Chemistry be held responsible for any errors or omissions in this *Accepted Manuscript* or any consequences arising from the use of any information it contains.

Cite this: DOI: 10.1039/c0xx00000x

www.rsc.org/xxxxxx

ARTICLE TYPE

Palladium encapsulated within magnetic hollow mesoporous TiO₂ spheres (Pd/Fe₃O₄@hTiO₂) as a highly efficient and recyclable catalysts for hydrodechlorination of chlorophenols

Le Zhang^{a,b}, Xingchun Zhou^b, Hongfei Huo^b, Wenzhu Li^b, Feng Li^b, Rong Li^{*b}

Received (in XXX, XXX) Xth XXXXXXXXX 20XX, Accepted Xth XXXXXXXXX 20XX
DOI: 10.1039/b000000x

Herein, we introduced a method to encapsulate Pd(0) within TiO₂ hollow mesoporous nanostructures. TiO₂ hollow spheres offer a number of advantageous characteristics, including low cost, low toxicity, relatively high photocatalytic activity and high chemical stability. In addition, it can also effectively avoid the agglomeration and precipitation of noble metal nanoparticles in the catalytic reaction. The catalyst was characterized by TEM, XRD, XPS, ICP and VSM. We found that the catalyst presented a high activity for HDC of 4-CP under mild reaction conditions. Beyond that, the catalyst could be easily regained by an external magnet from the reaction mixture and recycled seven times without any significant loss in activity.

1. Introduction

Developing high-performance and stable catalysts has become a hot area of research recently.^{1,2,3} Noble metal nanoparticles (NMNPs), especially Pd and Au, have been researched widely in recent years on account of their excellent catalytic performance in many chemical reactions, such as hydrogenation reactions,⁴ coupling reactions⁵ and oxidation reactions.⁶ It is generally believed that their shape, size, crystallinity and the surface state have large influence on the catalytic activity of NMNPs.⁷ Unhappily, NMNPs are easy to aggregate during the process of catalytic reaction, issuing in rapid decay of catalytic activity and stability.^{8,9} Therefore, to develop varieties of strategies to effectively synthesize and utilize NMNPs catalysts with satisfying dimensions and improved catalytic performance is a technologically significant and challenging issue.^{10,11,12}

Many evidences represented that hollow space have attracted considerable interest due to their high surface area, large void volume and low density.^{13,14,15} Core-shell structured materials with hollow space show a special type of complicated hybrids, which affords an efficient solution to prevent the undesirable aggregation, sintering, coalescence or corrosion/dissolution of entrapped catalytic species, for example, we can use shell to protect NMNPs. Meantime, diffusion and mass transfer of reactants could be speeded by the porous voids endowed by hollow space.^{16,17,18,19} In addition, nanostructured TiO₂ has attracted significant attention because of its beneficial properties for actual catalytic applications. TiO₂ hollow nanostructures consisting of nanoscale porous shells are highly satisfying because they possess high active surface area, reduced diffusion resistance and improved accessibility, which offer many new chances to the design of highly active nanostructured catalysts.²⁰ Except for good catalytic activity and high stability, recycling is

another important property for catalysts. As is well-known that the traditional separation techniques, such as filtration and centrifugation, are usually low efficiency and time-consuming, which is not adopted for recycling of catalysts.^{21,22} To solve this problem, magnetic nanoparticles, such as Fe₃O₄ nanoparticles, are utilized as this support materials because of their distinct physical properties and easy separation from reaction mixture by using an external magnet.^{23,24,25}

Based on above considerations, in this article, we described a mild route to synthesize Pd/Fe₃O₄@hTiO₂ catalyst with Pd/Fe₃O₄ nanoparticles resided inside the mesoporous spheres by using the colloidal SiO₂ spheres as the templates. The designed catalysts possess large magnetization, highly open and ordered mesopores, which shown excellent activity for HDC of 4-CP and could be easily recycled multiple times without visible decrease in the catalytic performance.

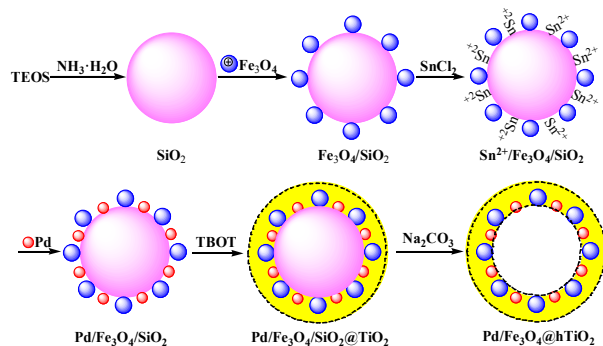
2. Experimental

2.1 Materials and reagents

Ammonia (NH₃·H₂O) solution (28 wt. %), tetraethoxysilane (TEOS), ethanol, triethylene glycol (TEG), tetrabutyl orthotitanate (TBOT), hydrochloric acid (HCl) (38 wt. %), N,N-dimethylformamide (DMF), triethylamine ((C₂H₅)₃N), ethyl acetate (CH₃COOC₂H₅) were purchased from Tianjing Chemical Reagent Co. Ferric acetylacetonate (Fe(acac)₃), SnCl₂, palladium chloride (PdCl₂), sodium formate (HCOONa), sodium acetate (CH₃COONa), sodium carbonate (Na₂CO₃), sodium hydroxide (NaOH) were bought from Aladdin Chemical Co., Ltd. 4-Chlorophenol (4-CP), 2-chlorophenol (2-CP), 3-chlorophenol (3-CP), and 2,4-dichlorophenol (2,4-DCP) are purchased from Lanzhou Aihua Chemical Company. All chemicals were of analytical grade and were used as received without further

purification.

2.2 Preparation of catalysts



Scheme 1. Scheme of the synthetic procedure for the preparation of Pd/Fe₃O₄@hTiO₂

The fabrication procedure involved six steps as shown in Scheme 1. Firstly, SiO₂ was prepared. Secondly, load Fe₃O₄ nanoparticles on surface of SiO₂. Thirdly, deposit Sn²⁺ onto the surface of SiO₂ nanospheres with Fe₃O₄ nanoparticles. Fourthly, load highly dispersed Pd nanoparticles onto the surface of SiO₂ nanospheres with Fe₃O₄ nanoparticles. Fifth, the Pd/Fe₃O₄/SiO₂@TiO₂ core-shell structures were prepared. Finally, the as-prepared nanocomposites were etched by Na₂CO₃ to remove the template. The amount of Pd in the obtained catalyst was found to be 2.26 wt. % based on ICP analysis.

2.2.1 Synthesis of SiO₂ nanospheres²⁶

In a typical synthesis, 4.5 mL of TEOS was rapidly added into a mixture solution of 62 mL ethanol, 25 mL H₂O and 1.5 mL NH₃·H₂O. After stirring for 2 h, the SiO₂ particles were collected by centrifugation and washed with ethanol and deionized water. This process was repeated three times before drying the SiO₂ particles at 50 °C.

2.2.2 Preparation of Fe₃O₄/SiO₂ composite²⁷

Firstly, 250mg SiO₂ particles and 60ml TEG were added into a three-necked flask (100ml), and then the three-necked flask was treated under ultrasonic to disperse uniformly. Secondly, 300mg Fe(acac)₃ was still added into the three-necked flask with magnetic stirring under the protection of N₂ at the same time. The system was warmed till boiling and kept for 30min, after cooling down to room temperature. Fe₃O₄ nanoparticles attached on the surface of SiO₂ nanospheres, were separated from the solution by an external magnet and washed several times with ethanol and distilled water until the pH value of the solution became approximately 7 before oven-dried at 50 °C for further use.

2.2.3 Preparation of Pd/Fe₃O₄/SiO₂ composite²⁸

200 mg Fe₃O₄/SiO₂ sphere powders was added to 35 mL distilled water and ultraphonic for 10 min as part A. 200 mg SnCl₂ was dissolved in 40 mL 0.02 M HCl solution as part B. Parts A and B were mixed together under ultraphonic condition. 2 h later, the precipitate was collected by centrifugation, followed by washing with distilled water five times, and dispersed into 50 mL distilled water. Then 50 mL 16 mg PdCl₂ was added into it. 30 min later, 20 mL of 0.15 M HCOONa solution was added, followed by stirring for 8 h. The suspension was separated from the solution by centrifugation, after washing with distilled water and ethanol for several times, the product dried in vacuum at 50 °C for further use.

2.2.4 Synthesis of Pd/Fe₃O₄@hTiO₂ catalysts²⁹

Typically, 70 mg Pd/Fe₃O₄/SiO₂ particles were dispersed in 100 mL ethanol and ultraphonic for 30 min. Then, 0.35 mL NH₃·H₂O was added to the suspension and continue to ultrasonic for 30min, afterward, 0.75 mL of TBOT was added dropwise in 5 min, and the reaction was allowed to proceed for 24 h at 45 °C under vigorous magnetic stirring. After that, the products separated by centrifugation and washed with distilled water and ethanol, respectively. The final product was dried in vacuum at 50 °C. Next, the Pd/Fe₃O₄@hTiO₂ was obtained by etching Pd/Fe₃O₄/SiO₂@TiO₂ spheres in 2M Na₂CO₃ aqueous solution for 8 h and washed five times with distilled water and dried.

2.3 Characterization of catalysts

The synthesized catalyst of Pd/Fe₃O₄@hTiO₂ was confirmed by corresponding characterization means. The morphology and microstructure of Pd/Fe₃O₄@hTiO₂ were characterized by transmission electron microscopy (TEM). The TEM images were obtained through Tecnai G2 F30 electron microscope operating at 300 kV. X-ray powder diffraction (XRD) measurements were carried out at room temperature and performed on a Rigaku D/max-2400 diffractometer using Cu-Kα radiation as the X-ray source in the 2θ range of 10-90°. X-ray photoelectron spectroscopy (XPS) was recorded on a PHI-5702 and the C1s line at 291.4 eV was used as the binding energy reference. Specific surface areas were calculated by the Brunauer–Emmett–Teller (BET) method and pore sizes by the Barrett–Joyner–Halenda (BJH) methods using Brunauer–Emmett–Teller (Tristar II 3020). Inductive coupled plasma atomic emission spectrometer (ICP-AES) analysis was conducted with Perkin Elmer (Optima-4300DV). Magnetic measurement of Pd/Fe₃O₄/SiO₂ nanoreactor and Pd/Fe₃O₄@hTiO₂ were investigated with a Quantum Design vibrating sample magnetometer (VSM) at room temperature in an applied magnetic field sweeping from 15 to 15 kOe. The conversions of the HDC reactions were estimated by gas chromatography-mass spectrometry GC-MS (P.E. AutoSystem XL).

2.4 Catalytic activity and recyclability

The HDC of 4-CP reaction was carried out in a 50 mL two-necked flask. In general, the catalyst (10mL, 2 mg·mL⁻¹), NaOH solution (10 mL, 0.05 M) and CP (10 mL, 0.05 M) were mixed in a 50 mL two-necked flask. The sample was collected at an interval of 10 min. The filtrate was extracted by CH₃COOC₂H₅, and then the reaction conversion of the HDC reaction was estimated by GC-MS. To evaluate the reusability of the Pd/Fe₃O₄@hTiO₂ nanocatalyst in the HDC reaction, the nanocatalyst was recovered by a magnet, washed with water, and dried in vacuum at room temperature. In general, the catalyst was redispersed in a new reaction system for subsequent catalytic experiments under the same reaction conditions. Moreover, the catalytic procedure was repeated seven times.

3. Results and discussion

3.1 Characterizations of the catalyst Pd/Fe₃O₄@hTiO₂

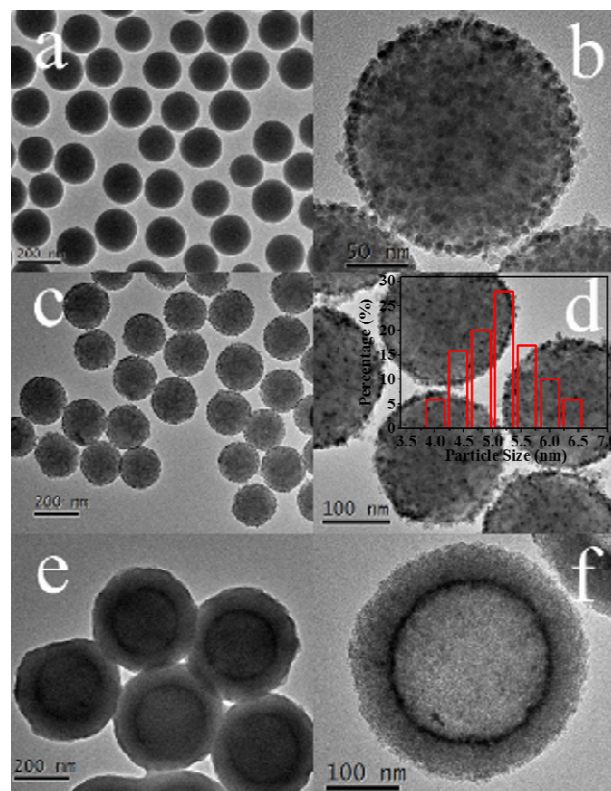


Fig. 1 TEM images of (a) SiO₂, (b) and (c) Fe₃O₄/SiO₂, (d) Pd/Fe₃O₄/SiO₂ (Inset pictures: size distribution histograms image of the Pd nanoparticles crystal structure in detail on Pd/Fe₃O₄/SiO₂), (e) Pd/Fe₃O₄/SiO₂@TiO₂, (f) Pd/Fe₃O₄@hTiO₂

The morphologies and structures of the products at different synthetic steps were observed by TEM. Fig. 1a shows the TEM image of SiO₂ nanospheres, in which well dispersed particles with average diameter about 200 nm could be observed clearly. Both fig. 1b and 1c show the TEM images of the Fe₃O₄/SiO₂ composite, and the Fe₃O₄ particles with an average size of about 10 nm are uniformly distributed on the surface of the SiO₂ nanospheres. Fig. 1d displays the TEM image of Pd/Fe₃O₄/SiO₂ nanospheres with Pd and Fe₃O₄ nanoparticles well dispersed on the outer surfaces of SiO₂ nanospheres. The sizes of Pd nanoparticles are estimated to be 5 nm. Fig. 1e shows the TEM images of Pd/Fe₃O₄/SiO₂@TiO₂ nanospheres. The Pd/Fe₃O₄/SiO₂@TiO₂ nanospheres with the diameter of ~320nm have relatively smooth surfaces and better dispersion. The SiO₂ core was removed using concentrated Na₂CO₃ aqueous solution, leaving only Pd and Fe₃O₄ nanoparticles inside the hollow TiO₂, resulting in the formation of Pd/Fe₃O₄/SiO₂@hTiO₂ hollow spheres. The TEM images of Pd/Fe₃O₄@hTiO₂ shown in Fig. 1f. It clearly displays the hollow mesoporous structures of TiO₂ with a shell thickness of ~40 nm.

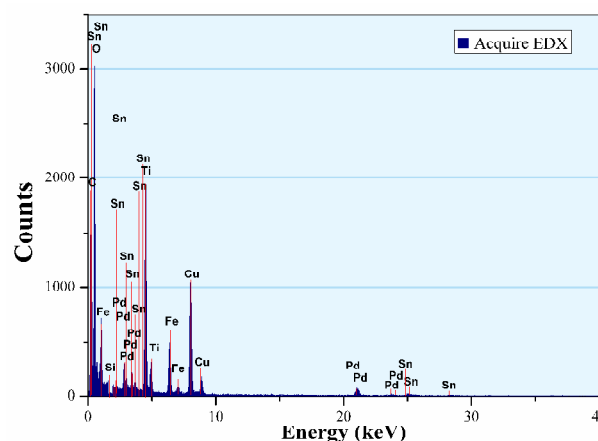


Fig. 2 EDX spectrum of Pd/Fe₃O₄@hTiO₂

The elemental composition of the Pd/Fe₃O₄@hTiO₂ samples was determined by EDX analysis. The result shown in Fig. 2 revealed that the as-prepared products contain Pd, Fe, Cu, Ti, C, Si, Sn and O. Among these elements, Cu and C are generally influenced by the copper network support films and their degree of oxidation, Pd, Fe and Ti signals result from the Pd/Fe₃O₄@hTiO₂. And from the EDX result, the signal of Si element has not been found, revealed that the SiO₂ was totally removed.

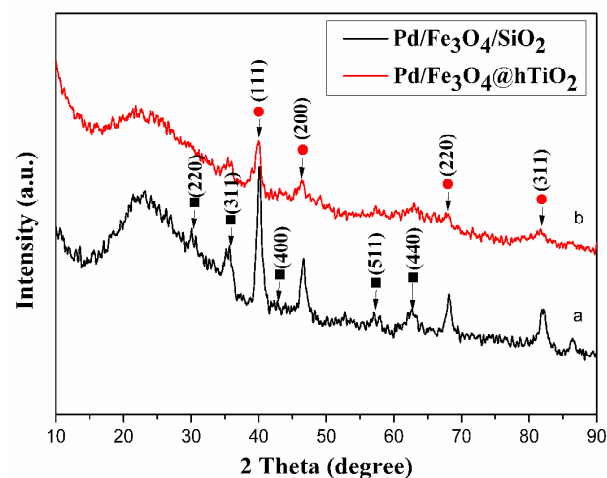


Fig. 3 XRD patterns of (a) Pd/Fe₃O₄/SiO₂, (b) Pd/Fe₃O₄@hTiO₂

(● represents Pd nanoparticles; ■ represents Fe₃O₄ nanoparticles)

Fig. 3 shows the XRD patterns between 10 and 90° of the samples. Fig. 3a shows the wide angle XRD pattern of Pd/Fe₃O₄/SiO₂ composites. Five diffraction peaks appear at 2θ=30.6°, 35.8°, 43.4°, 57.5° and 63.2°, corresponding to the reflections of (220), (311), (400), (511) and (440) crystal planes of Fe₃O₄, respectively. Fig. 3b shows the wide angle XRD pattern of Pd/Fe₃O₄@hTiO₂ composites. Four diffraction peaks appear at 2θ=40.1°, 46.5°, 68.0° and 82.6°, corresponding to the reflections of (111), (200), (220) and (311) crystal planes of Pd, respectively. Meanwhile, the result indicating the crystalline structure of the support was well maintained in the Pd samples. The average crystallite size of Pd nanoparticles in Pd/Fe₃O₄@hTiO₂ were calculated using Scherrer's equation, is about 5 nm.

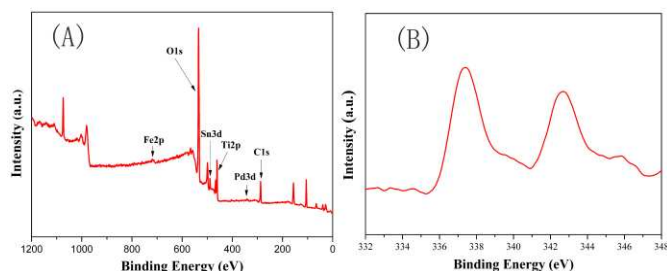


Fig. 4 (A) XPS spectrum of the elemental survey scan of Pd/Fe₃O₄@hTiO₂ and (B) high-resolution spectrum of Pd 3d

Fig. 4 shows the XPS spectrum of the synthesized Pd/Fe₃O₄@hTiO₂ nanoreactor. Peaks corresponding to O, C, Fe, Pd, Ti and Sn are observed. However, typical peaks of Sn, Fe and Pd elements are not obviously detected, which indicates that Sn, Fe and Pd particles have been coated by TiO₂, since the analysis depth of XPS is only several nanometers. To ascertain the oxidation state of the Pd, XPS studies are carried out. The XPS signature of Pd 3d doublet for the Pd nanoparticles is given in the fig.4(B). The Pd 3d_{3/2} and Pd 3d_{5/2} peaks appeared at 342.6 and 337.2 eV respectively are the characteristic peaks for the metallic Pd(0). We can see that there is no oxidation state of Pd species in the catalyst. In the experiment, the reducing agent is excessive so that the Pd(II) could be reduced into Pd(0) completely, which is beneficial for the reaction.

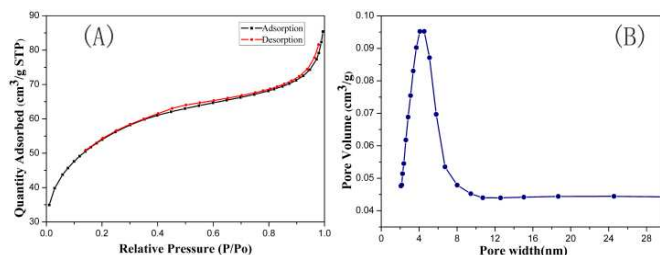


Fig. 5 (A) N₂ adsorption/desorption isotherms of the Pd/Fe₃O₄@hTiO₂ (B) the corresponding pore diameter distribution

Fig. 5 shows nitrogen adsorption/desorption isotherms and the corresponding pore size distribution of the Pd/Fe₃O₄@hTiO₂. The BET surface area and single point total pore volume is 180 m²·g⁻¹ and 0.13 cm³·g⁻¹, respectively, which are considerably large values because the solid core and Pd nanoparticles have been included in the calculations. The average BJH (Barrette Joynere Halenda) pore diameter calculated from the adsorption branch of the isotherm and the desorption branch of the isotherm are 4.5 nm. On the basis of above analysis, it can be concluded that these data further identified the hollow mesoporous structure of the synthesized Pd/Fe₃O₄@hTiO₂ catalyst.

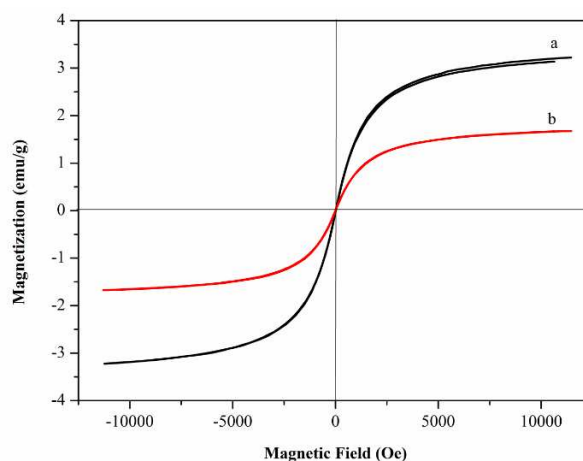


Fig. 6 Room temperature magnetization curves of (a) Pd/Fe₃O₄/SiO₂, (b) Pd/Fe₃O₄@hTiO₂

Magnetic measurements were carried out by employing VSM at room temperature. The magnetization curves measured for Pd/Fe₃O₄/SiO₂ and Pd/Fe₃O₄@hTiO₂ are compared in Fig. 6. There is no hysteresis in the magnetization for the two tested nanoparticles. It can be seen that the values of the saturation magnetization are 3.22 emu·g⁻¹ for Pd/Fe₃O₄/SiO₂ and 1.68 emu·g⁻¹ for Pd/Fe₃O₄@hTiO₂ respectively. The decrease of the saturation magnetization suggests the presence of some Pd particles inside the uniformly pore of hollow mesoporous spheres. Even with this reduction in the saturation magnetization, the catalyst still can be efficiently separated easily from the solution with the help of an external magnetic force.

3.2 Catalytic activity for HDC of 4-CP

The catalytic activity of the Pd/Fe₃O₄@hTiO₂ catalyst was established by the HDC of 4-CP under a mild condition. The HDC of 4-CP was negligible without catalyst or in the presence of pure hollow magnetic mesoporous TiO₂ spheres at the same conditions, which shows that the presence of NMNPs are indispensable for high catalytic activity. As Diaz et al.³⁰ explained in a previous work the route of 4-CP HDC proceeded through a set of series-parallel reactions where 4-CP gives rise to phenol and cyclohexanone (CYC) being this last also produced from phenol hydrogenation. Compared with the reactant 4-CP, the two products detected are low toxic and useful as intermediates in production of high value-added chemicals. In this work, the high selectivity product phenol was observed. The low selectivity of HDC of 4-CP performed in fixed bed reactor³¹ or under a high H₂ pressure condition,³⁰ such as: Pd/C catalyzed HDC of 4-CP with the conversion of 93% and the selectivity of 85% were reported by J. Rodriguez, which formic acid as hydrogen source in continuous stirred-tank reactor.³² Pd/Al₂O₃ as HDC catalyst was also studied by J. Juan³¹, in fixed bed reactor with the conversion was 87% and the selectivity 62%, respectively. Compared with reports above mentioned, in our reaction, a batch stirred tank reactor was used and only H₂ was flowing phase. The main production was phenol and less than 0.1% CYC was detected after 2 h reaction time. These differences may be caused by the using of different reaction systems. This result was agreed with the study using same reaction system

which phenol as major product was detected.

Table 1 Effect of different solvents and different bases^a

<chem>Oc1ccc(Cl)cc1</chem> $\xrightarrow[\text{Base, Solvent, 25 }^\circ\text{C}]{\text{Pd/HMMS, H}_2(1\text{atm})}$ <chem>Oc1ccccc1</chem> + HCl			
Entry	Base	Solvent	Yield
1	NaOH	C ₂ H ₅ OH	12.2%
2	NaOH	CH ₃ COOC ₂ H ₅	22.8%
3	NaOH	DMF	4.1%
4	NaOH	H ₂ O	99.9%
5	Na ₂ CO ₃	H ₂ O	72.9%
6	CH ₃ COONa	H ₂ O	97.2%
7	(C ₂ H ₅) ₃ N	H ₂ O	93.9%

^a Conditions: 4-CP (0.5 mmol, 64.3 mg), base (0.5 mmol), solvent (30 mL), catalyst (20 mg), H₂ balloon (30 mL·min⁻¹), 25 °C, 2 h.

The HDC reaction mechanism was described below: H₂ adsorbed on the active site of the Pd/Fe₃O₄@hTiO₂ catalyst was activated into two hydrogen atoms which combined with 4-CP also adsorbed on the surface of the catalyst. The C-Cl bond of 4-CP was attacked by the active hydrogen atoms to form phenol.³³

The abovementioned results clearly indicated that the Pd/Fe₃O₄@hTiO₂ nanocatalysts exhibited the favorable catalytic performance toward HDC of 4-CP. The catalytic properties and recyclability were evaluated by performing HDC of 4-CP. Pd/Fe₃O₄@hTiO₂ was used as a probe catalyst to optimize the reaction conditions and to catch the best reaction conditions. Therefore, a series of reactions was performed using several bases and solvents to obtain the best possible combination (Table 1). In order to prevent the poisoning of the catalysts, hydrochloric acid (HCl) produced during the HDC process was neutralized by the bases added to the reaction system.³⁴ Therefore, NaOH was first used as a neutralizer to test different solvents (Table 1, entries 1–4). The yields of phenol in C₂H₅OH, CH₃COOC₂H₅, DMF, and H₂O were 12.2, 22.8, 4.1, and 99.9%, respectively. These low yields of phenol obtained in the abovementioned organic solvents were mainly ascribed to the low solubility of NaOH that leads to the poisoning of the nanocatalyst. As a result, based on the above-mentioned results, H₂O was considered to be the best solvent for the HDC of 4-CP. To further optimize the reaction conditions, different bases were tested in the aqueous solution (Table 1, entries 4–7). The results indicated that the yield of phenol in the HDC reaction was significantly affected by the basicity of the neutralizer for HCl as reported by Zahara M. de Pedro.^{35,36} The highest reaction rate and phenol yield were achieved when the process was carried out in strong base (NaOH) solution. In comparison, when a weak base (Na₂CO₃, CH₃COONa, NH₃·H₂O, or (C₂H₅)₃N) was employed, a low yield of phenol was obtained under the same reaction conditions (Table 1). Hence, NaOH was considered as the optimized base for HDC reaction. Thus, the catalytic properties of Pd/Fe₃O₄@hTiO₂ in the HDC of 4-CP were investigated using NaOH and H₂O as the optimized base and solvent, respectively.

Table 2 Catalytic HDC of different substrates over the Pd/Fe₃O₄@hTiO₂ nanocatalyst^a

Entry	Reactants	Main products	Yield
1	<chem>Oc1ccc(Cl)cc1</chem>	<chem>Oc1ccccc1</chem>	99.9%
2	<chem>Oc1ccc(Cl)cc1</chem>	<chem>Oc1ccccc1</chem>	99.9%
3 ^b	<chem>Oc1c(Cl)ccc(Cl)c1</chem>	<chem>Oc1ccccc1</chem>	68.6%

^a Conditions: chlorophenol (0.5 mmol), base (1 equiv.), solvent (30 mL), catalyst (20 mg), H₂ (30 mL·min⁻¹), 25 °C, 2 h. ^b 2equiv. of NaOH.

In order to investigate the application of the Pd/Fe₃O₄@hTiO₂ nanocatalyst for HDC of chlorophenols, we also studied the HDC of 2-CP, 3-CP and 2,4-dichlorophenol (2,4-DCP) catalyzed by the Pd/Fe₃O₄@hTiO₂ nanocatalyst and the corresponding results were listed in Table 2. The values listed in Table 2 revealed that 3-CP and 2-CP were also almost completely transformed into phenol within 2 h. Except, the low yields of phenol obtained from 2,4-DCP.^{37,38} The reason was ascribed probably to the electronic and steric hindrance of 2,4-DCP. Compared with the literature^{33,39}, this synthesized catalyst Pd/Fe₃O₄@hTiO₂ exhibited comparable or much better catalytic activity for HDC.

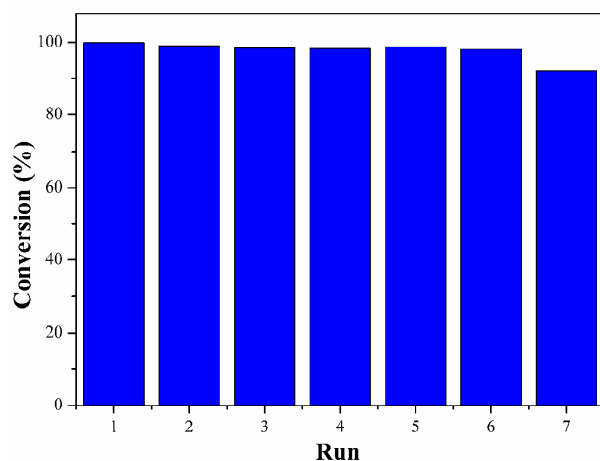


Fig. 7 The recycling experiments of the catalyst Pd/Fe₃O₄@hTiO₂.

The recyclability of Pd/Fe₃O₄@hTiO₂ catalyst was further investigated. After completion of the reaction, the catalyst was recovered from the reaction mixture by using an external magnet. The recovered catalyst was washed with ethanol for several times, and dried at room temperature. As illustrated in Fig. 7, the catalyst was reused for at least seven times without a significant loss of activity.

4. Conclusions

In conclusion, we describe a method to encapsulate Pd(0) within

TiO₂ hollow mesoporous nanostructures. The designed Pd/Fe₃O₄@hTiO₂ nanoreactors possess hollow core/mesoporous shell structures, high catalytic activity and magnetic recyclability properties. The designed catalyst exhibits high activity for HDC of 4-CP under mild conditions and could be recovered in a facile manner from the reaction mixture and recycled seven times without any loss in activity. Furthermore, the method is also extended to introduce other NMNPs including Au, Ag, Pt, and their bimetallic nanoparticles inside TiO₂ hollow mesoporous nanostructures to prepare other new catalysts.

Acknowledgements

The authors are grateful to Projects in Gansu Province Science and Technology Pillar Program.

Notes and references

^aDepartment of Chemical Engineering, Jiuquan College of Vocational Technology, Jiuquan, 735000, Gansu, China

^bCollege of Chemistry and Chemical Engineering Lanzhou University, The Key Laboratory of Catalytic engineering of Gansu Province, Lanzhou, 730000, Gansu, China

- D. R. Rolison, *Science*, 2003, **299**, 1698-1701.
- A. T. Bell, *Science*, 2003, **299**, 1688-1691.
- N. Zhang and Y.-J. Xu, *Chemistry of Materials*, 2013, **25**, 1979-1988.
- M. Crespo-Quesada, F. Cárdenas-Lizana, A.-L. Dessimoz and L. Kiwi-Minsker, *ACS Catalysis*, 2012, **2**, 1773-1786.
- A. Fihri, M. Bouhrara, B. Nekoueshahraki, J.-M. Basset and V. Polshettiwar, *Chemical Society Reviews*, 2011, **40**, 5181-5203.
- L. Kesavan, R. Tiruvalam, M. H. A. Rahim, M. I. bin Saiman, D. I. Enache, R. L. Jenkins, N. Dimitratos, J. A. Lopez-Sanchez, S. H. Taylor, D. W. Knight, C. J. Kiely and G. J. Hutchings, *Science*, 2011, **331**, 195-199.
- R. Güttel, M. Paul, C. Galeano and F. Schüth, *Journal of Catalysis*, 2012, **289**, 100-104.
- R. Narayanan and M. A. El-Sayed, *Journal of the American Chemical Society*, 2003, **125**, 8340-8347.
- A. Corma and H. Garcia, *Chemical Society Reviews*, 2008, **37**, 2096-2126.
- J. Lee, J. C. Park and H. Song, *Advanced Materials*, 2008, **20**, 1523-1528.
- K. Yoon, Y. Yang, P. Lu, D. Wan, H.-C. Peng, K. Stamm Masias, P. T. Fanson, C. T. Campbell and Y. Xia, *Angewandte Chemie International Edition*, 2012, **51**, 9543-9546.
- J. Ge, Q. Zhang, T. Zhang and Y. Yin, *Angewandte Chemie International Edition*, 2008, **47**, 8924-8928.
- J. Tian, L. Yuan, M. Zhang, F. Zheng, Q. Xiong and H. Zhao, *Langmuir*, 2012, **28**, 9365-9371.
- T. Yao, T. Cui, X. Fang, J. Yu, F. Cui and J. Wu, *Chemical Engineering Journal*, 2013, **225**, 230-236.
- Y. Li, X. Li, Y. Li, H. Liu, S. Wang, H. Gan, J. Li, N. Wang, X. He and D. Zhu, *Angewandte Chemie International Edition*, 2006, **45**, 3639-3643.
- C.-H. Lin, X. Liu, S.-H. Wu, K.-H. Liu and C.-Y. Mou, *The Journal of Physical Chemistry Letters*, 2011, **2**, 2984-2988.
- S. Ikeda, S. Ishino, T. Harada, N. Okamoto, T. Sakata, H. Mori, S. Kuwabata, T. Torimoto and M. Matsumura, *Angewandte Chemie International Edition*, 2006, **45**, 7063-7066.
- J. Liu, S. Z. Qiao, S. Budi Hartono and G. Q. Lu, *Angewandte Chemie International Edition*, 2010, **49**, 4981-4985.
- Z. Liang, A. Susha and F. Caruso, *Chemistry of Materials*, 2003, **15**, 3176-3183.
- J. B. Joo, M. Dahl, N. Li, F. Zaera and Y. Yin, *Energy & Environmental Science*, 2013, **6**, 2082-2092.
- V. Polshettiwar, R. Luque, A. Fihri, H. Zhu, M. Bouhrara and J.-M. Basset, *Chemical Reviews*, 2011, **111**, 3036-3075.
- T. Yao, T. Cui, H. Wang, L. Xu, F. Cui and J. Wu, *Nanoscale*, 2014, **6**, 7666-7674.
- S. Shylesh, V. Schünemann and W. R. Thiel, *Angewandte Chemie International Edition*, 2010, **49**, 3428-3459.
- K. Mori, N. Yoshioka, Y. Kondo, T. Takeuchi and H. Yamashita, *Green Chemistry*, 2009, **11**, 1337-1342.
- Y. Zhu, L. P. Stubbs, F. Ho, R. Liu, C. P. Ship, J. A. Maguire and N. S. Hosmane, *ChemCatChem*, 2010, **2**, 365-374.
- T. Zhang, Q. Zhang, J. Ge, J. Goebel, M. Sun, Y. Yan, Y.-s. Liu, C. Chang, J. Guo and Y. Yin, *The Journal of Physical Chemistry C*, 2009, **113**, 3168-3175.
- L. Y. Xia, M. Q. Zhang, C. e. Yuan and M. Z. Rong, *Journal of Materials Chemistry*, 2011, **21**, 9020-9026.
- L.-S. Zhong, J.-S. Hu, Z.-M. Cui, L.-J. Wan and W.-G. Song, *Chemistry of Materials*, 2007, **19**, 4557-4562.
- H. Liu, S. Ji, Y. Zheng, M. Li and H. Yang, *Chinese Journal of Chemical Engineering*, 2013, **21**, 569-576.
- E. Díaz, J. A. Casas, A. F. Mohedano, L. Calvo, M. A. Gilarranz and J. J. Rodríguez, *Industrial & Engineering Chemistry Research*, 2008, **47**, 3840-3846.
- E. Díaz, J. A. Casas, A. F. Mohedano, L. Calvo, M. A. Gilarranz and J. J. Rodríguez, *Industrial & Engineering Chemistry Research*, 2009, **48**, 3351-3358.
- L. Calvo, M. A. Gilarranz, J. A. Casas, A. F. Mohedano and J. J. Rodríguez, *Journal of Hazardous Materials*, 2009, **161**, 842-847.
- Z. Dong, X. Le, C. Dong, W. Zhang, X. Li and J. Ma, *Applied Catalysis B: Environmental*, 2015, **162**, 372-380.
- C. Sun, Z. Wu, Y. Mao, X. Yin, L. Ma, D. Wang and M. Zhang, *Catalysis Letters*, 2011, **141**, 792-798.
- Z. M. de Pedro, E. Diaz, A. F. Mohedano, J. A. Casas and J. J. Rodríguez, *Applied Catalysis B: Environmental*, 2011, **103**, 128-135.
- C. Xia, Y. Liu, J. Xu, J. Yu, W. Qin and X. Liang, *Catalysis Communications*, 2009, **10**, 456-458.
- J. Zhou, K. Wu, W. Wang, Z. Xu, H. Wan and S. Zheng, *Applied Catalysis A: General*, 2014, **470**, 336-343.
- S. Gómez-Quero, F. Cárdenas-Lizana and M. A. Keane, *Journal of Catalysis*, 2013, **303**, 41-49.
- Y. Liu, X. Li, X. Le, W. Zhang, H. Gu, R. Xue and J. Ma, *New Journal of Chemistry*, 2015, **39**, 4519-4525.